OPEN ACCESS
CellPress

Cell Reports
Article

Selective Activation of mTORC1 Signaling Recapitulates Microcephaly, Tuberous Sclerosis, and Neurodegenerative Diseases

Hidetoshi Kassai,[1] Yuki Sugaya,[2] Shoko Noda,[1] Kazuki Nakao,[1,3] Tatsuya Maeda,[4] Masanobu Kano,[2] and Atsu Aiba[1,*]
[1]Laboratory of Animal Resources, Center for Disease Biology and Integrative Medicine, Graduate School of Medicine, The University of Tokyo, Tokyo 113-0033, Japan
[2]Department of Neurophysiology, Graduate School of Medicine, The University of Tokyo, Tokyo 113-0033, Japan
[3]Laboratory for Animal Resources and Genetic Engineering, RIKEN Center for Developmental Biology, Kobe 650-0047, Japan
[4]Institute of Molecular and Cellular Biosciences, The University of Tokyo, Tokyo 113-0032, Japan
*Correspondence: aiba@m.u-tokyo.ac.jp
http://dx.doi.org/10.1016/j.celrep.2014.04.048

SUMMARY

Mammalian target of rapamycin (mTOR) has been implicated in human neurological diseases such as tuberous sclerosis complex (TSC), neurodegeneration, and autism. However, little is known about when and how mTOR is involved in the pathogenesis of these diseases, due to a lack of animal models that directly increase mTOR activity. Here, we generated transgenic mice expressing a gain-of-function mutant of mTOR in the forebrain in a temporally controlled manner. Selective activation of mTORC1 in embryonic stages induced cortical atrophy caused by prominent apoptosis of neuronal progenitors, associated with upregulation of HIF-1α. In striking contrast, activation of the mTORC1 pathway in adulthood resulted in cortical hypertrophy with fatal epileptic seizures, recapitulating human TSC. Activated mTORC1 in the adult cortex also promoted rapid accumulation of cytoplasmic inclusions and activation of microglial cells, indicative of progressive neurodegeneration. Our findings demonstrate that mTORC1 plays different roles in developmental and adult stages and contributes to human neurological diseases.

INTRODUCTION

Mammalian (or mechanistic) target of rapamycin (mTOR) is an evolutionarily conserved serine/threonine kinase that regulates cellular metabolism in response to multiple environmental stimuli, such as growth factors and amino acids, as well as energy availability (Laplante and Sabatini, 2012; Wullschleger et al., 2006). mTOR functions in two structurally distinct protein complexes, named mTOR complex 1 (mTORC1) and mTORC2. Activation of the mTORC1 pathway facilitates protein synthesis via phosphorylation of p70 S6 kinase (S6K1 and S6K2) and eukaryotic initiation factor 4-binding protein (4EBP1 and 4EBP2). Concurrently, activated mTORC1 suppresses protein degradation by inhibiting the autophagic pathway. Thus, mTORC1 signaling integrates a wide variety of cellular processes, including cell growth, proliferation, and survival, by coupling and balancing anabolic and catabolic states.

The importance of mTOR for cellular function is reflected in the association of dysregulated mTOR signaling with human diseases such as cancer, diabetes, and obesity (Cornu et al., 2013; Laplante and Sabatini, 2012; Yang et al., 2012). Accumulating evidence demonstrates that mTOR also plays a key role in quiescent cells, especially in neurons. Loss of function of mTOR signaling causes impairment of axon guidance, dendritic arborization, and synaptic plasticity in cultured neurons (Jaworski and Sheng, 2006; Swiech et al., 2008), and hypomyelination in mice with conditional knockout of the small G-protein Rheb1, a proximal activator of mTORC1 (Yamagata et al., 1994; Zou et al., 2011). In the human CNS, dysregulation of mTOR signaling is observed in various neurological and neuropsychiatric disorders, such as neurodegenerative diseases (Bové et al., 2011; Reith et al., 2011), tuberous sclerosis complex (TSC) (Orlova and Crino, 2010), fragile X syndrome (Busquets-Garcia et al., 2013; Sharma et al., 2010), and autism (Sato et al., 2012; Tsai et al., 2012). Neurodegenerative diseases, such as Alzheimer's, Huntington's, and Parkinson's diseases, are characterized by accumulation of misfolded protein aggregates called cytoplasmic inclusions, which leads to cellular damage and a functional loss of neurons (Bové et al., 2011). Administration of rapamycin to a mouse model of neurodegenerative diseases ameliorates neuronal cell death (Ravikumar et al., 2004), suggesting that activation of mTOR is involved in the progression of these diseases, presumably by suppressing autophagic degradation of inclusions. TSC is an autosomal-dominant genetic disorder caused by mutations in either the *TSC1* or *TSC2* gene (Orlova and Crino, 2010). TSC1 and TSC2 negatively control mTORC1 activity by forming a heterodimer that acts as a GTPase-activating protein for Rheb. TSC pathology is characterized by nonmalignant tumors called hamartomas in many organs. The neurological manifestation of TSC is hamartomatous lesions called cortical tubers, subependymal nodules, and subependymal giant cell astrocytomas. These

brain lesions are assumed to induce neuropsychiatric symptoms such as epileptic seizure, autism, and mental retardation in TSC patients.

Importantly, as is the case with human cancer, mTOR signaling is consistently hyperactivated but not suppressed in mTOR-related neurological disorders. In the case of TSC, conditional knockout mice deficient in *Tsc1* or *Tsc2* in various brain regions have been developed so as to recapitulate TSC pathogenesis. In the cerebral cortex, conditional knockout mice of *Tsc1* have shown epileptic seizures, premature death, and abnormal cytoarchitecture of the forebrain, including the cerebral cortex and hippocampus (Carson et al., 2012; Magri et al., 2011; Meikle et al., 2007; Way et al., 2009; Zhou et al., 2011). However, because mTORC1 can be regulated independently of TSC1/2, the extent to which mTOR activation is involved in the pathogenic mechanisms of TSC has been unclear. For example, AMP-activated protein kinase directly phosphorylates raptor, a component of mTORC1, leading to inhibition of mTORC1 signaling (Gwinn et al., 2008). Akt also regulates mTORC1 activity in a TSC1/2-independent manner by phosphorylating PRAS40, an mTORC1 inhibitor (Sancak et al., 2007; Vander Haar et al., 2007; Wang et al., 2007). In addition, mTOR function in the developing brain, where neuronal progenitors actively undergo proliferation, may differ from that in the mature brain, where postmitotic neurons exert diverse neurological functions. Therefore, it has been difficult to address when and how mTOR activation is important for brain development and functions, as well as the pathogenesis of human diseases.

In this study, we demonstrate that mTORC1 signaling plays different physiological roles in developing and mature brains. We established transgenic (Tg) mice lines carrying mTOR kinase with gain-of-function mutations that direct selective activation of the mTORC1 pathway in a spatially and temporally controlled manner. Mutant mice expressing active mTOR kinase in the embryonic cortex displayed progressive apoptotic cell death of neuronal progenitors, resulting in cortical atrophy. In marked contrast, mTORC1 activation in postmitotic neurons in both juvenile and adult mice led to cortical hypertrophy and severe epileptic seizures. Concomitantly, cytoplasmic inclusions rapidly accumulated in the cortical neurons after chronic activation of mTORC1, indicative of neurodegeneration. Our data provide direct evidence that stage-specific activation of mTORC1 signaling faithfully recapitulates human microcephaly, TSC, and neurodegenerative diseases.

RESULTS

Embryonic Activation of the mTOR Pathway

For chronic activation of the mTOR pathway, we used a hyperactive mutant of rat mTOR kinase ($mTOR^{SL1+IT}$), which harbors four point mutations in the FRB (FKBP12-rapamycin binding) and kinase domains, and is tagged with the FLAG epitope at its N terminus (Ohne et al., 2008). In cultured cells, active mTOR keeps enhanced kinase activity specifically toward mTORC1 substrates such as S6K1 and 4EBP1 even under starvation conditions, but its kinase activity is sensitive to rapamycin. In contrast, the kinase activity toward the mTORC2 substrate Akt1 is hardly retained under starvation conditions (Ohne et al., 2008). Hyperactivation of the mTORC1 pathway, but not mTORC2, was also observed in the Tg mice used in this study (see Figures 4D, S4A, and S4B). We established a line of Tg mice in which $mTOR^{SL1+IT}$ is placed under control of the ubiquitous CAG promoter, but its expression was subjected to interference by the *loxP*-flanked *neo* gene (*CAG-*$mTOR^{SL1+IT}$; Figure 1A). Therefore, active mTOR can be conditionally expressed upon excision of the *neo* gene in response to Cre-*loxP* recombination. These Tg mice (*CAG-*$mTOR^{SL1+IT}$/+) were crossed with Emx1-cre knockin mice ($Emx1^{cre/+}$) to obtain *CAG-*$mTOR^{SL1+IT}$/+; $Emx1^{cre/+}$ mice (Kassai et al., 2008). Emx1-cre mice express Cre recombinase exclusively in the dorsal telencephalon (Figure 1B) as early as embryonic day 10 (E10). Emx1-lineage neuronal progenitor cells in the dorsal telencephalon give rise to almost all projection neurons as well as a subset of glial cells in the cerebral cortex and hippocampus in adulthood. Thus, active mTOR is assumed to be expressed in these brain regions during cortical development in *CAG-*$mTOR^{SL1+IT}$/+; $Emx1^{cre/+}$ mice. Hereafter, *CAG-*$mTOR^{SL1+IT}$/+; $Emx1^{cre/+}$ mice are referred to as Emx1-mTOR Tg mice. *CAG-*$mTOR^{SL1+IT}$/+ mice were used for the experimental control animals.

Decreased Cortical Size in Emx1-mTOR Tg Mice

Emx1-mTOR Tg mice were obtained at the expected Mendelian ratio and survived to adulthood without gross abnormalities in their appearance. However, the cerebral cortex of Emx1-mTOR Tg mice was remarkably atrophied in adulthood (Figures 1C and 1D). Despite a reduction in its size, the cortical structure was almost preserved with a six-layered cytoarchitecture, as revealed by immunohistochemical distribution of Cux1- and FoxP2-positive neurons located at layers II/III and layer VI, respectively (Figures 1E and 1F). The hippocampus of Emx1-mTOR Tg mice was also smaller than that of control mice (Figures 1D and S1), but other brain regions lacking Cre expression were almost unaffected by the genotype (Figures 1C and 1D). Interestingly, protein expression of active mTOR was undetectable in the cortical lysate of Emx1-mTOR Tg mice in adulthood (Figure S2), suggesting that most of the active mTOR-expressing cells underwent cell death during corticogenesis. When the Emx1-mTOR Tg mice were examined at embryonic stages, cortical atrophy was already obvious at E12 without affecting the morphology of lateral and medial ganglionic eminences, where cortical interneurons are generated (Figures 2A–2C). These results indicate that embryonic activation of mTORC1 reduces the cortical size during corticogenesis.

Neuronal Progenitor Cell Death in Emx1-mTOR Tg Cortex

Given that the cortical size was decreased by the expression of active mTOR, we examined cell proliferation and survival of neuronal progenitor cells in Emx1-mTOR Tg cortex at E12. Neuronal progenitor cells in M phase of the cell cycle divide at the apical surface of the ventricular zone. These dividing cells can be marked by phosphorylated histone H3 (pH3) immunoreactivity. The number of pH3-positive cells was not significantly different between control and Emx1-mTOR Tg cortices (Figures 2D–2F), indicating that proliferation of neuronal progenitor cells was not affected by the activation of mTORC1 pathway. Next,

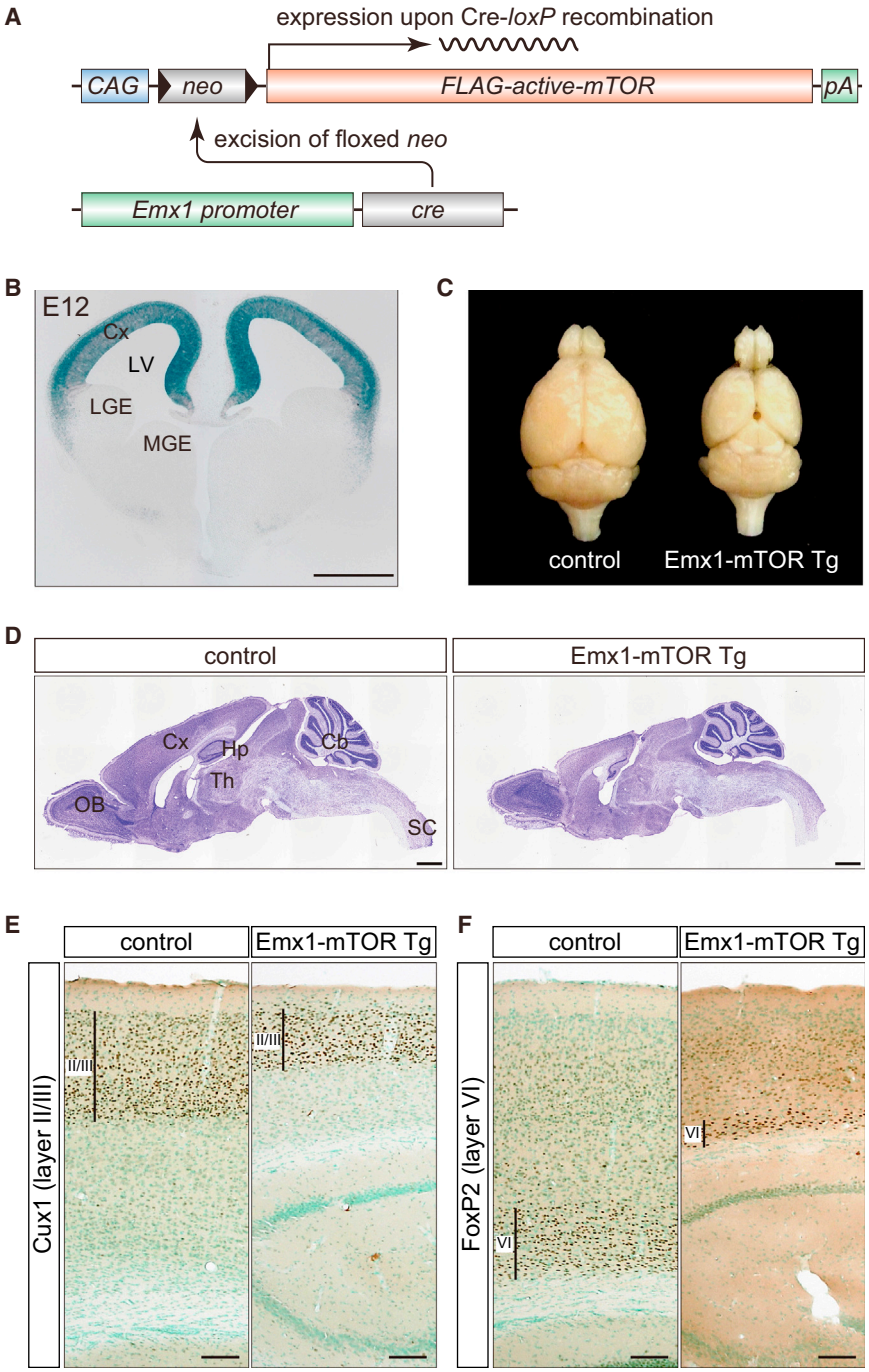

Figure 1. Activation of the mTOR Pathway in Embryonic Dorsal Telencephalon

(A) Transgenic strategy for conditional expression of active mTOR kinase by the Cre-*loxP* system. Excision of the floxed *neo* gene by Cre recombinase induces active mTOR expression driven by the CAG promoter. The *cre* gene is inserted into the endogenous *Emx1* locus for expression in the embryonic dorsal telencephalon of Emx1-cre knockin mice.

(B) Expression patterns of Cre recombinase in Emx1-cre knockin mice. Emx1-cre knockin mice were crossed with Cre-activatable *lacZ* reporter mice, and brain sections were stained with X-gal. Cre expression was readily detectable and restricted in the dorsal telencephalon at E12. Note that Cre expression is absent in the lateral ganglionic eminence (LGE) and medial ganglionic eminence (MGE), where cortical interneurons are generated and migrate into the neocortex.

(C and D) Decreased cortical size of Emx1-mTOR Tg brain in adulthood. Control and Emx1-mTOR Tg brains were fixed and isolated at 8 weeks of age. Sagittal brain sections were stained with cresyl violet.

(E and F) Thinned but normal cortical layer in Emx1-mTOR Tg mice. Cortical sections at 8 weeks of age were immunostained with Cux1 (E, layer II/III) or FoxP2 (F, layer VI). Cb, cerebellum; Cx, cerebral cortex; Hp, hippocampus; LGE, lateral ganglionic eminence; LV, lateral ventricle; MGE, medial ganglionic eminence; OB, olfactory bulb; SC, spinal cord; Th, thalamus.

Scale bars, 500 μm (B), 1 mm (D) and 100 μm (E and F). See also Figures S1 and S2.

to determine the cause of neuronal cell loss, we examined apoptotic cell death by immunohistochemical staining of cleaved caspase 3 (CC3). A significant increase of CC3 immunoreactivity was detected in Emx1-mTOR Tg cortex compared with the control at E12 (Figures 2G–2I). The CC3-positive area almost overlapped with pyknotic nuclei (Figure 2H), another characteristic feature of apoptosis. The apoptotic cells were also merged with FLAG-positive cells (Figure S3), indicating that active mTOR is expressed in the dying cells. As CC3-positive cells with pyknotic nuclei were mainly localized at the subventricular zone (SVZ) of the cortex, we tested whether the survival of SVZ progenitors was sensitive to activation of mTORC1 signaling. As expected, the number of Tbr2-positive SVZ progenitors was significantly decreased in Emx1-mTOR Tg mice (Figures 2J–2L). Together, these results indicate that activation of the mTORC1 pathway promotes apoptotic cell death of neuronal progenitors without affecting their proliferation during corticogenesis.

We explored mTOR-regulated downstream effectors that triggered the apoptotic cell death of neuronal progenitors. Hypoxia-inducible factor 1α (HIF-1α) is a transcription factor that is responsible for oxygen sensing (Sharp and Bernaudin, 2004) and is implicated in apoptotic signaling (Carmeliet et al., 1998). HIF-1α is rapidly ubiquitinylated and degraded by the proteasome under normoxic conditions. In hypoxia, HIF-1α is stabilized and forms a complex with HIF-1β to activate expression of target genes related to angiogenesis and apoptosis (Sharp and Bernaudin, 2004). Activation of the mTOR pathway is involved in

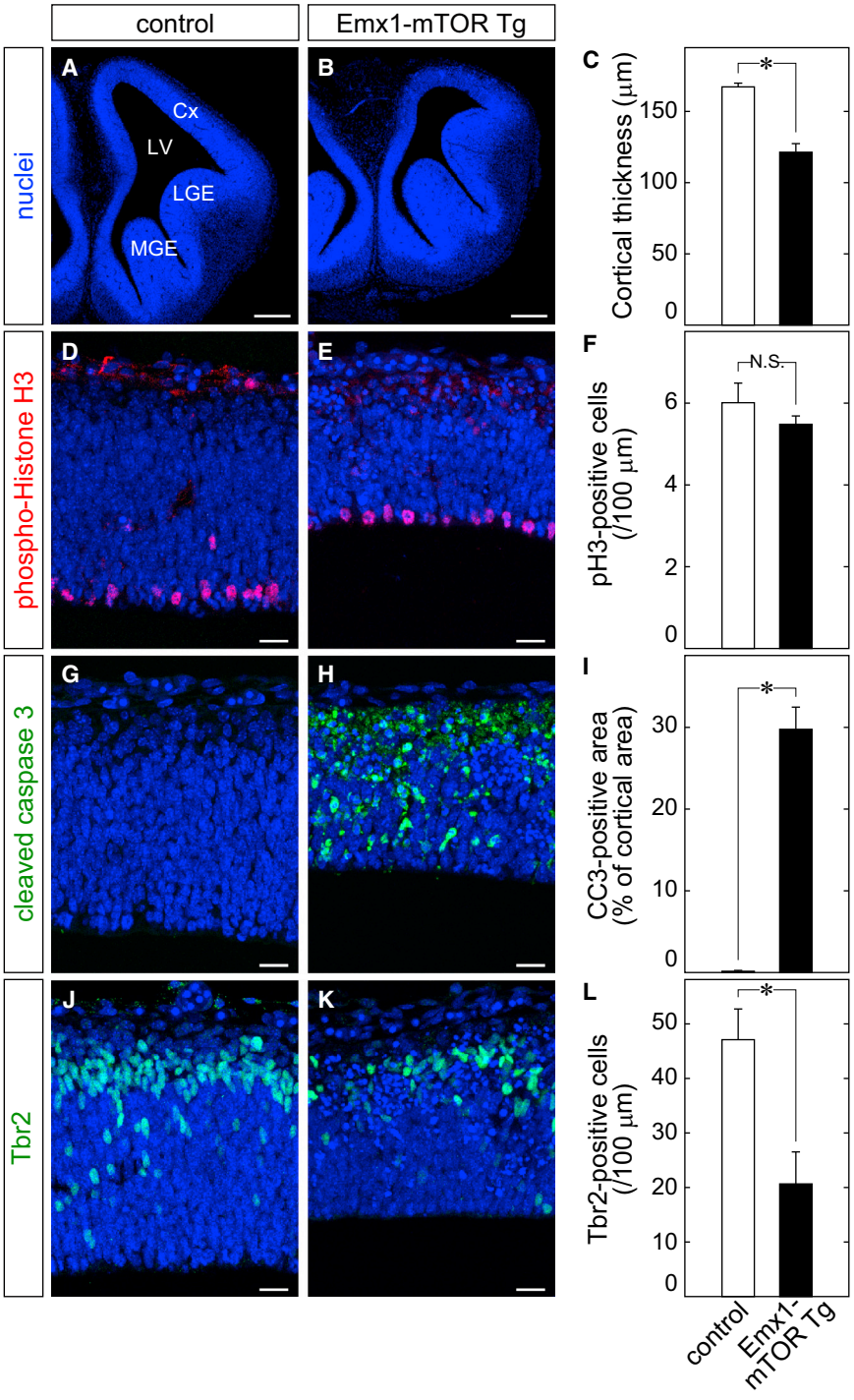

Figure 2. Apoptotic Cell Death of Neuronal Progenitors by Embryonic Activation of the mTOR Pathway

(A–C) Reduced cortical thickness in Emx1-mTOR Tg embryo. Coronal sections from control (A) and Emx1-mTOR Tg (B) brains at E12 were stained with TO-PRO-3.

(D–F) Normal proliferation of neuronal progenitors in Emx1-mTOR Tg cortex. M phase progenitor cells of E12 cortex were marked with anti-phospho-histone H3 antibody. The number of M phase progenitors at the ventricular surface was not significantly different between two genotypes.

(G–I) Increased apoptotic cell death of neuronal progenitors by activation of the mTOR pathway. CC3-positive cells were markedly increased in Emx1-mTOR Tg cortex at E12 (H), but were almost undetectable in control cortex (G). The CC3-immunopositive area was quantified as the percentage relative to the corresponding total cortical area (I).

(J–L) Loss of Tbr2-positive SVZ progenitors in Emx1-mTOR Tg mice. Tbr2-positive cells were quantified as the number of cells found in a certain width (100 μm) of the cortex along the medial-lateral axis. Values are means ± SD. *$p < 0.005$, Student's t test ($n = 3$). N.S., not significant.

Scale bars, 200 μm (A and B) and 20 μm (D, E, G, H, J, and K). See also Figure S3.

oxygen-independent regulation of HIF-1α expression by increasing both the translation and stabilization of HIF-1α (Land and Tee, 2007). In Emx1-mTOR Tg cortex at E12, we found that the expression of HIF-1α was remarkably elevated compared with the control (Figures 3A, 3D, and 3H). HIF-1α expression almost overlapped with CC3-positive apoptotic cells (Figures 3D–3F), suggesting that neuronal progenitor cell death may be mediated by HIF-1 signaling. To further confirm activation of the HIF-1 pathway, we examined the expression of the HIF-1 target gene in E12 cortex. We observed prominent induction of p21 (also termed cyclin-dependent kinase inhibitor 1A) protein expression in Emx1-mTOR Tg cortex in the corresponding cortical area where HIF-1α expression was upregulated (Figures 3G and 3H). Thus, HIF-1 induction through mTORC1 activation may contribute to increased apoptotic cell death in Emx1-mTOR Tg mice during corticogenesis.

Activation of mTORC1 Signaling in Postmitotic Neurons

Because mTORC1 activation in the embryonic cortex leads to apoptotic progenitor cell death, we established another line of Tg mice to analyze mTOR function in a spatially and temporally controlled manner. In the new line of Tg mice, *mTOR*$^{SL1+lT}$ is linked to tetracycline-responsive element (TRE), and thus its expression can be regulated by tetracycline-controlled transactivator (tTA; Figure 4A). These Tg mice (*TRE-mTOR*$^{SL1+lT}$/+) were crossed with CaMKII-tTA Tg mice (*CaMKII-tTA*/+) in which tTA is driven by the CaMKII promoter and is expressed in postmitotic excitatory neurons in the forebrain from the late embryonic or early postnatal period

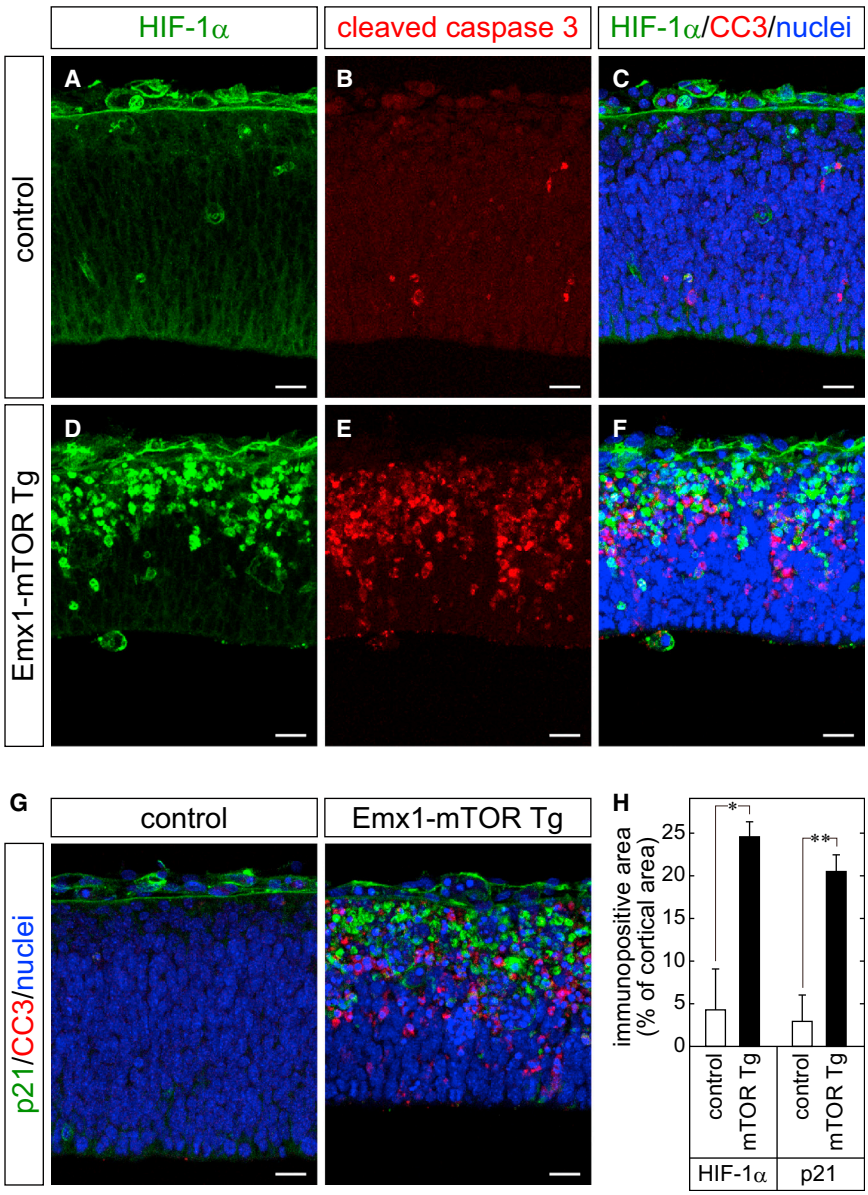

Figure 3. Altered HIF-1 Signaling by mTORC1 Activation in the Embryonic Cortex

(A–F) Increased expression of HIF-1α in Emx1-mTOR Tg cortex. Coronal sections from control (A–C) and Emx1-mTOR Tg brains (D–F) at E12 were immunostained with antibodies against HIF-1α (green in A and D) and CC3 (red in B and E). HIF-1α and CC3 signals are merged with nuclear staining (C and F).

(G) Induction of p21 expression in Emx1-mTOR Tg mice. Expression of p21, the HIF-1 target gene, was markedly increased and overlapped with the CC3-positive area in Emx1-mTOR Tg mice at E12.

(H) Quantification of HIF-1α and p21 signals in the embryonic cortex. The immunopositive area of each protein was expressed as a percentage of the corresponding total cortical area. *$p < 0.01$, **$p < 0.005$, Student's t test ($n = 3$). Scale bars, 20 μm.

(Mayford et al., 1996). Without doxycycline administration, *TRE-mTOR*$^{SL1+IT}$*/+; CaMKII-tTA/+* mice (hereafter designated CaMKII-mTOR Dox(−) Tg mice) exhibited severe growth retardation from postnatal day 10 (P10) and died at 15–20 days of age (Figure 4B).

In CaMKII-mTOR Dox(−) Tg cortex, active mTOR expression was increased postnatally and reached the maximum expression level around P10 (Figure 4C). Hyperactivation of the mTORC1 pathway was confirmed by enhanced phosphorylation level of S6K1 at Thr389 in the cortical lysate from CaMKII-mTOR Dox(−) Tg mice compared with that from the control (Figure 4D). The regional specificity of active mTOR expression was analyzed by immunohistochemical localization of phosphorylated ribosomal S6 protein, a downstream target of S6K1. We detected intense staining for phosphorylated Ser-235/236 of S6 protein in the cerebral cortex and hippocampus of CaMKII-mTOR Dox(−) Tg brain (Figures 4E and 4F). These expression profiles are consistent with spatiotemporal distribution of tTA expression in CaMKII-tTA Tg mice (Mayford et al., 1996), and thus the mTORC1 pathway should be activated in postmitotic neurons of the forebrain in CaMKII-mTOR Dox(−) Tg mice. It is noteworthy that the phosphorylation level of Akt at Ser-473 in CaMKII-mTOR Dox(−) Tg cortex was not different from that in the control (Figure 4D), suggesting that the mTORC2 pathway was almost unaffected by the expression of active mTOR.

Impaired Neuronal Migration and Cell Size Regulation by mTORC1 Activation

Previous studies showed that loss of the *Pten* or *Tsc1* gene in the telencephalon leads to postnatal hypertrophy of the cerebral cortex and cortical neurons (Carson et al., 2012; Groszer et al., 2001; Magri et al., 2011; Meikle et al., 2007; Way et al., 2009; Zhou et al., 2011), presumably due to activation of mTOR signaling. We assessed whether direct and selective activation of mTORC1 pathway alters the cortical size and structure in CaMKII-mTOR Tg Dox(−) mice. Despite the growth retardation, CaMKII-mTOR Dox(−) Tg displayed cortical hypertrophy at P12 (Figures 4G–4J). Both the cortical thickness (control: 0.86 ± 0.06 mm; Tg: 1.36 ± 0.06 mm; Figures 4G, 4I, and 4K) and soma size of cortical neurons (control: 62.7 ± 11.4 μm^2, Tg: 145.4 ± 33.5 μm^2; Figures 4H, 4J, and 4L) were prominently increased in CaMKII-tTA Dox(−) Tg mice. In addition, cortical lamination was disrupted in CaMKII-tTA Dox(−) Tg mice, as indicated by the immunohistochemical localization of Cux1-positive layer II/III neurons

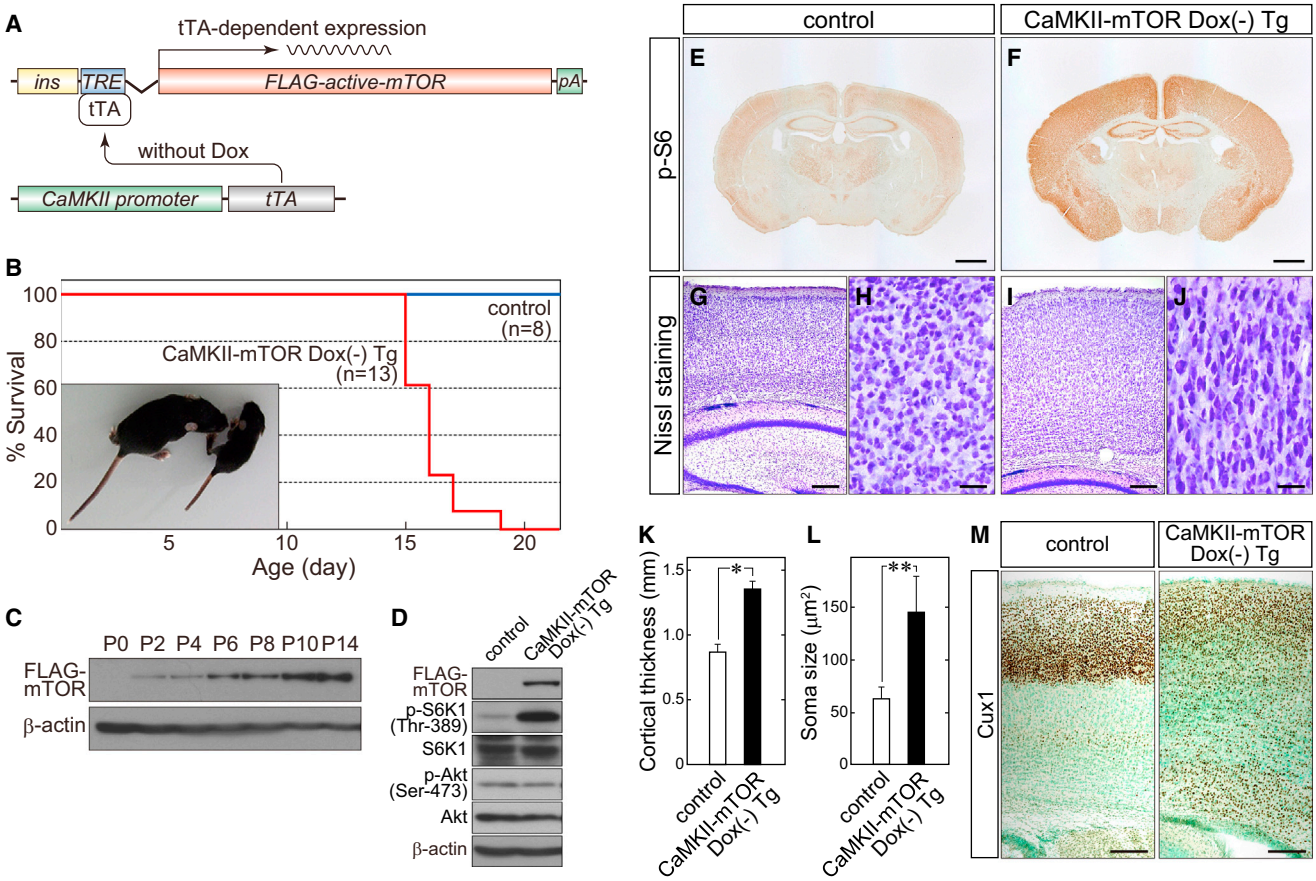

Figure 4. Activation of the mTORC1 Pathway in Postmitotic Neurons in Immature Mice

(A) Transgenic strategy for conditional expression of active mTOR kinase by the Tet-Off system. Expression of active mTOR depends on binding of tTA to the TRE promoter. The CaMKII promoter drives tTA expression in postmitotic excitatory neurons of the forebrain.

(B) Cumulative survival curves for CaMKII-mTOR Dox(−) Tg (red line) and control (blue line) mice. Inset: typical appearances of control (left) and CaMKII-mTOR Dox(−) Tg mice (right).

(C) Age-dependent change in active mTOR expression in CaMKII-mTOR Dox(−) Tg mice. Cortical lysates from CaMKII-tTA Dox(−) Tg mice at the designated ages were prepared and immunoblotted with antibodies against FLAG and β-actin.

(D) Selective activation of the mTORC1 pathway in CaMKII-tTA Dox(−) Tg mice. Increased phosphorylation of S6K1 at Thr-389 was seen in the protein extract from CaMKII-mTOR Dox(−) Tg cortex at P14 compared with that from the control. However, phosphorylation of Akt at Ser-473 was not affected by active mTOR expression.

(E and F) Distribution of phosphorylated S6 protein in control and CaMKII-mTOR Dox(−) Tg brains. The regional specificity of activation of the mTORC1 pathway was examined by immunohistochemistry of phosphorylated S6 protein at Ser-235/236. In CaMKII-mTOR Dox(−) Tg mice, an increased number of immuno-positive neurons were detected in the cerebral cortex and hippocampus.

(G–J) Cortical hypertrophy in CaMKII-mTOR Dox(−) Tg mice. Shown are nissl-stained coronal sections of cerebral cortices from control and CaMKII-mTOR Dox(−) Tg mice at P15. Both cortical thickness (G and I) and neuronal soma size (H and J) of CaMKII-mTOR Dox(−) Tg mice were increased compared with those of the control.

(K and L) Quantification of cortical thickness and neuronal soma size of control and CaMKII-mTOR Dox(−) Tg mice. Values are means ± SD. *$p < 0.001$ ($n = 3$), **$p < 10^{-59}$ (control: $n = 201$; Tg: $n = 132$), Student's t test.

(M) Abnormal cortical structure in CaMKII-mTOR Dox(−) Tg mice. Cux1-positive cortical layer II/III neurons were scattered throughout the cortex in CaMKII-mTOR Dox(−) Tg mice, indicative of impaired neuronal migration.

Scale bars, 1 mm (E and F), 200 μm (G and I), 50 μm (H and J), and 100 μm (M).

sparsely distributed throughout the cortex (Figure 4M). These results demonstrate that activation of the mTORC1 pathway in postmitotic neuron results in dysregulation of neuronal cell size and migration, leading to macrocephaly with abnormal cortical cytoarchitecture.

Neuronal hypertrophy and impaired neuronal migration by mTORC1 activation were also confirmed by in utero electroporation experiments. When cortical progenitors at E14 were transfected with EGFP-expressing plasmid, EGFP-labeled neurons migrated from the ventricular zone to the pial surface of the cortex (Figure 5A). When cotransfected with wild-type mTOR-expressing plasmid, the EGFP-labeled neurons normally migrated to the pial surface (Figure 5B), suggesting that overexpression of mTOR per se does not affect the neuronal migration

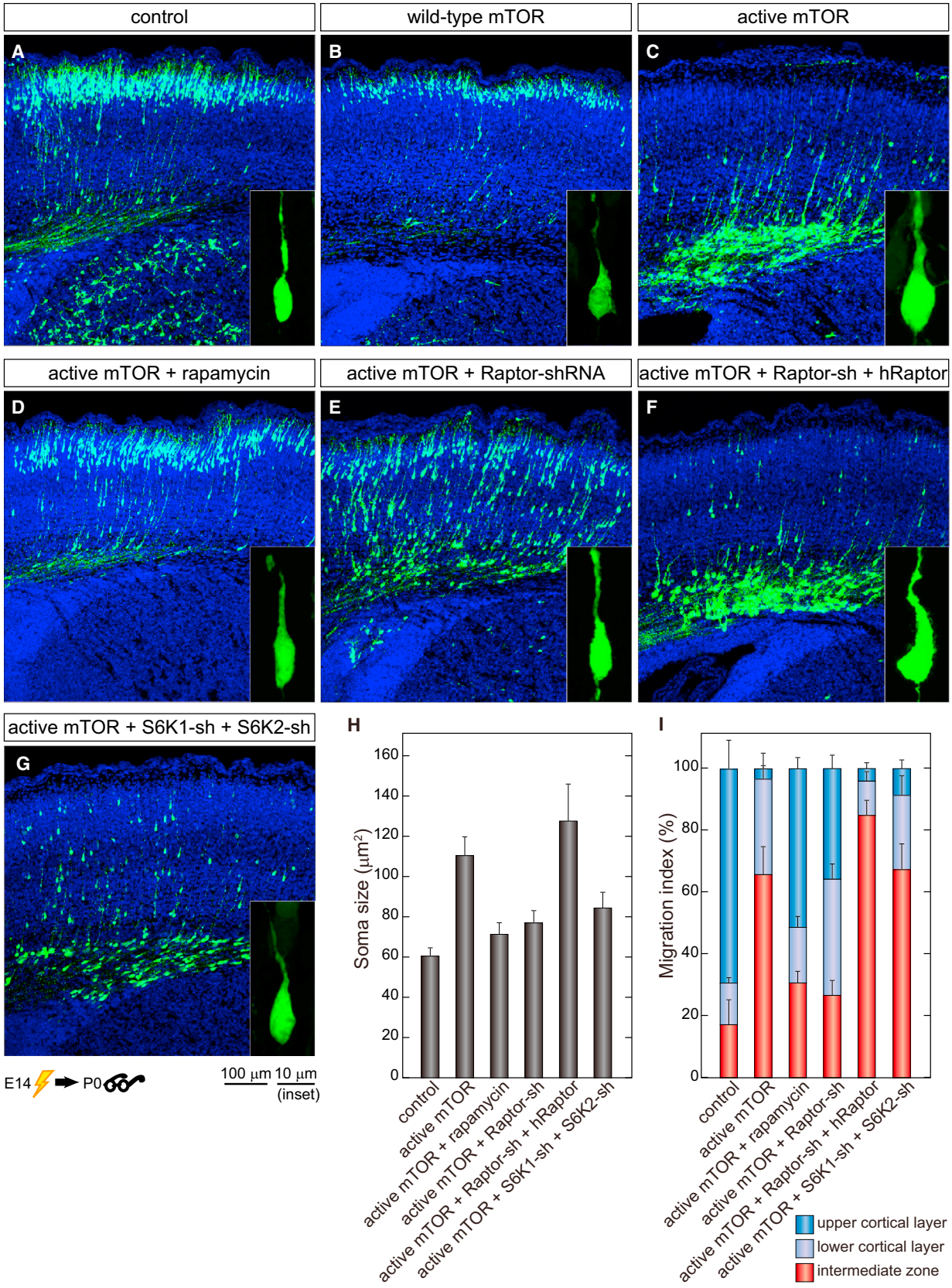

(legend on next page)

or cell size. In sharp contrast, cortical neurons expressing active mTOR failed to migrate to the pial surface, remaining in the intermediate zone (Figure 5C). In addition, active mTOR-expressing neurons showed increased soma size compared with the control (inset in Figures 5A–5C). After transfection of active mTOR into the embryonic cortex, acute administration of rapamycin (5 mg/kg) to the pregnant mother restored both impaired neuronal migration and neuronal hypertrophy (Figure 5D). Furthermore, knockdown of raptor by small hairpin RNA (shRNA) also rescued both impaired neuronal migration and increased cell size induced by active mTOR expression (Figure 5E). The target specificity of raptor knockdown was confirmed by the coexpression of knockdown-resistant human raptor, which reversed the phenotypes to abnormal migration and enlarged soma (Figure 5F). Therefore, we can conclude that impaired neuronal migration and cell size regulation can be attributed largely to specific activation of mTORC1 signaling. As for neuronal hypertrophy, we identified S6K1 and S6K2 as possible targets of mTORC1 signaling for neuronal cell size regulation. Neuronal hypertrophy induced by active mTOR expression was rescued by knockdown of S6K1 and S6K2 (Figure 5G), suggesting that the mTORC1-S6K pathway may be important for neuronal cell size regulation.

Activation of the mTORC1 Pathway in Adulthood

Given that CaMKII-mTOR Dox(−) Tg mice exhibited growth retardation and postnatal lethality, we tried to activate the mTORC1 pathway in adulthood. To avoid developmental perturbation in the forebrain, we suppressed active mTOR expression by doxycycline administration until 3 weeks of age in Tg mice (Figure 6A). Hereafter, these mice are referred to as CaMKII-mTOR Dox3w Tg mice. *TRE-mTOR*$^{SL1+lT}$/+ mice that received doxycycline in the same way as the CaMKII-mTOR Dox3w Tg mice were used as experimental control animals. After withdrawal of doxycycline at 3 weeks of age, we could detect a gradual increase of active mTOR expression in the cerebral cortex of CaMKII-mTOR Dox3w Tg mice after 5 weeks of age (Figure 6C). Excessive phosphorylation of S6K1 was obvious at 6 weeks of age (Figure 6C), and hyperphosphorylation of S6 protein was restricted to the forebrain, including the cerebral cortex and hippocampus, in CaMKII-mTOR Dox3w Tg mice (Figures 6D and 6E). In contrast, the phosphorylation level of Akt at Ser-473 was not changed by active mTOR expression or rapamycin administration (Figures S4A and S4B). Therefore, the mTORC1 pathway, but not mTORC2, was spatiotemporally hyperactivated by doxycycline-regulated expression of active mTOR in CaMKII-mTOR Dox3w Tg mice.

Along with active mTOR expression, CaMKII-mTOR Dox3w Tg mice showed hypoactivity from 6 weeks of age, and all of them died between 6 and 7 weeks of age (Figure 6B). Similarly to CaMKII-mTOR Dox(−) Tg mice, CaMKII-mTOR Dox3w Tg mice showed cortical hypertrophy (Figures 6F–6K) with thickened cerebral cortex (Figures 6F, 6H, and 6J) and enlarged neuronal soma (Figures 6G, 6I, and 6K) at 6–7 weeks of age. Unlike CaMKII-mTOR Dox(−) Tg mice, the cortical lamination was almost preserved, as shown by the distribution of Cux1-positive layer II/III neurons properly located in the upper layer of the cortex (Figure 6L). These results demonstrate that activation of mTORC1 pathway in adulthood provokes macrocephaly without affecting the arrangement of the cortical layer during brain development.

Epileptic Seizures in CaMKII-mTOR Tg Mice

We explored a direct cause of lethality of CaMKII-mTOR Dox3w Tg mice by closely observing their behavior, especially during epileptic seizures, which are frequently seen in TSC patients. We observed frequent spontaneous seizures in CaMKII-mTOR Dox3w Tg mice 3–4 weeks after withdrawal of doxycycline. Seizures were characterized by unilateral forelimb clonus followed by bilateral forelimb clonus and falling (Movies S1 and S2). During the seizures, local field potentials (LFPs) recorded from the bilateral parietal cortices of freely moving CaMKII-mTOR Dox3w Tg mice showed rhythmic burst discharges lasting tens of seconds (Figure 7A). In addition, we could observe clear differences in LFPs between the right and left cortices during seizures (Figures 7A and 7B), indicating that abnormal neuronal discharges could be localized during the course of seizures, as reported in patients with TSC (Bebin et al., 1993). During the interictal period, active exploration was associated with bilateral synchronous theta oscillation of the LFP in CaMKII-mTOR Dox3w Tg mice, which was almost similar to that in control mice (Figure 7C). However, multifocal, large interictal spikes were frequently observed in CaMKII-mTOR Dox3w Tg mice (Figures 7D and 7E), but not in the control. These results suggest that the characteristic patterns of LFP during ictal and interictal periods in CaMKII-mTOR Dox3w Tg mice are similar to those in patients with TSC. It should be noted that hypertrophy of the CaMKII-mTOR Dox3w Tg cortex was suppressed by chronic administration of doxycycline or rapamycin (Figures S4C and S4D). Administration of doxycycline or rapamycin also inhibited epileptic seizures and postnatal lethality (data not shown).

Figure 5. Impaired Neuronal Migration and Increased Neuronal Cell Size by mTORC1 Activation

(A–C) Cortical neurons expressing EGFP or wild-type mTOR migrated appropriately near the pial surface of the cortex with normal cell size (A and B), whereas expression of active mTOR mutant resulted in impaired neuronal migration (C) and increased cell size (C, inset).

(D) Administration of rapamycin after introduction of active mTOR mutant completely rescued both impaired migration and increased cell size.

(E) Knockdown of raptor also rescued both impaired migration and increased cell size.

(F) The target specificity of raptor knockdown was confirmed by coexpression of knockdown-resistant human raptor, which abolished rescued phenotypes. Together, these data clearly demonstrate the specific involvement of mTORC1 in both neuronal migration and cell size regulation.

(G) Knockdown of S6K1 and S6K2 restored increased cell size to the normal state, indicating that the hyperactivated mTOR-S6K pathway impaired neuronal cell size regulation.

(H) Quantification of neuronal soma size. Values are means ± SD (n = 50 from 4 mice).

(I) Quantification of distribution of cortical neurons. Values are means ± SD (n = 8 slices from 4 mice)

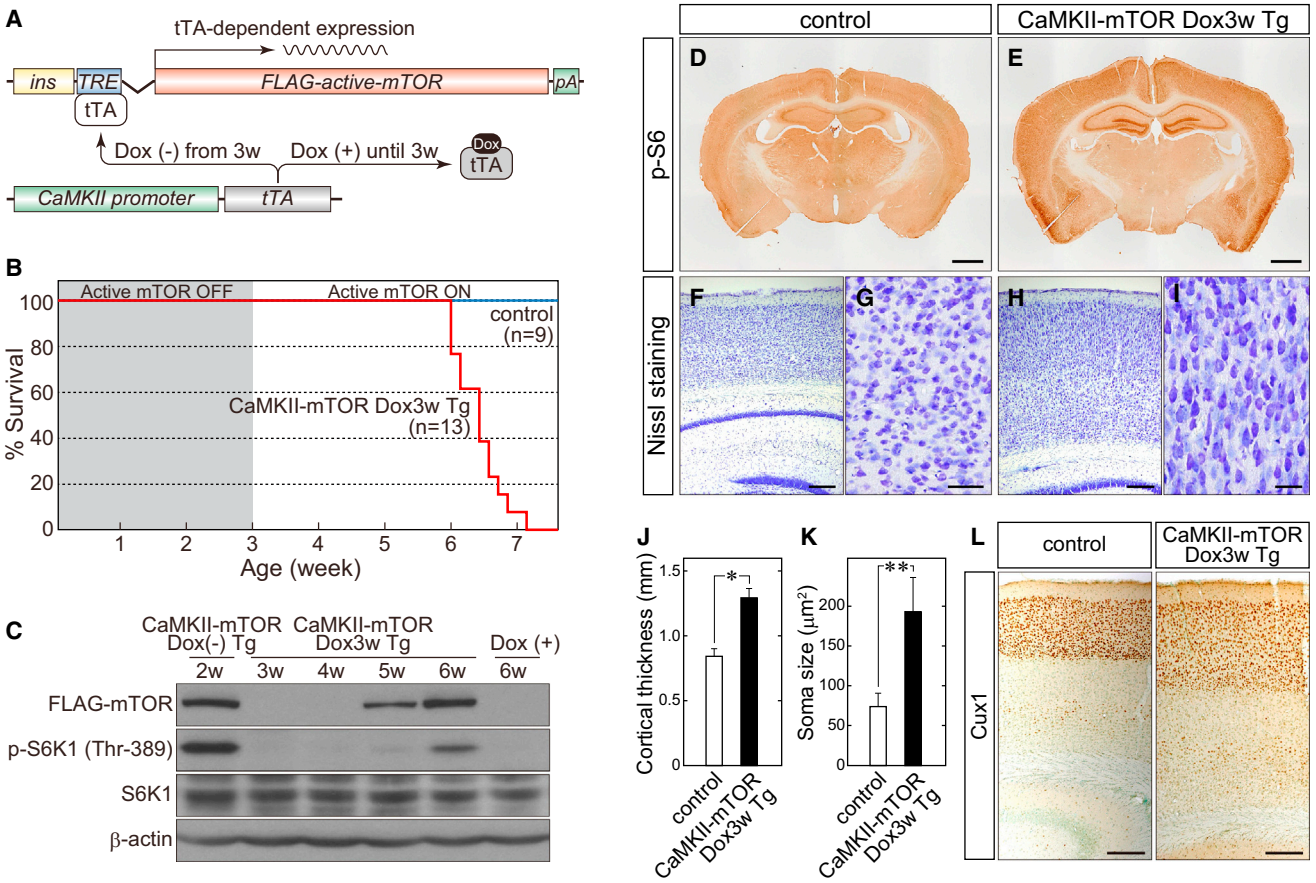

Figure 6. Activation of the mTORC1 Pathway in Adulthood

(A) Schematic diagram for reversible expression of active mTOR in CaMKII-mTOR Tg mice. Administration of Dox until 3 weeks of age prevents tTA from binding to TRE, silencing active mTOR expression. Withdrawal of Dox reactivates tTA binding to TRE, thereby inducing active mTOR expression in adulthood.

(B) Cumulative survival curves for CaMKII-mTOR Dox3w Tg (red line) and control (blue line) mice.

(C) Time-course expression profile of active mTOR protein. Cortical lysates at indicated age were immunoblotted with antibodies against FLAG, p-S6K1, S6K1, and β-actin. Dox (+) indicates CaMKII-mTOR Tg mice that were continuously administered Dox.

(D and E) Distribution of phosphorylated S6 protein in control and CaMKII-mTOR Dox3w Tg brains. Enhanced phosphorylation of S6 protein at Ser-235/236 was observed in the forebrain of CaMKII-mTOR Dox3w Tg mice.

(F–I) Nissl-stained coronal sections of cerebral cortices from control and CaMKII-mTOR Dox3w Tg mice at 7 weeks of age. Similar to what was observed in CaMKII-mTOR Dox(−) Tg mice, both cortical thickness (F and H) and neuronal soma size (G and I) were increased in CaMKII-mTOR Dox3w Tg mice.

(J and K) Quantification of cortical thickness and neuronal soma size of control and CaMKII-mTOR Dox3w Tg mice. Values are means ± SD. *$p < 10^{-4}$ (n = 3), **$p < 10^{-105}$ (control: n = 247; Tg: n = 201), Student's t test.

(L) Normal cortical layering in CaMKII-mTOR Dox3w Tg mice. Despite cortical hypertrophy, Cux1-positive cortical neurons were located properly at layers II/III in CaMKII-mTOR Dox3w Tg mice.

Scale bars, 1 mm (D and E), 200 μm (F and H), 50 μm (G and I), and 100 μm (L). See also Figure S4.

Therefore, these phenotypes can be attributed largely to hyperactivation of the mTORC1 pathway.

CaMKII-mTOR Dox(−) Tg mice also displayed spontaneous behavioral seizures around 2 weeks of age, accompanied by abnormal LFPs similar to those observed in CaMKII-mTOR Dox3w Tg mice (Figure S5; Movies S3 and S4). These were sometimes followed by tonic extension of four limbs toward the caudal direction. This tonic seizure lasted for several minutes, and although some mice gradually recovered, other mice died without recovery. Therefore, activation of the mTORC1 pathway in the forebrain is sufficient to induce fatal epileptic seizures.

Neurodegeneration of Cortical Neurons in CaMKII-mTOR Tg Mice

As embryonic activation of the mTORC1 pathway leads to apoptotic cell death of neuronal progenitors, we tested whether mTORC1 signaling in postmitotic neurons regulates neuronal cell survival. We did not detect excessive immunoreactivity of CC3 in CaMKII-tTA Dox(−) Tg cortex at P12 (Figure S6), suggesting that mTORC1 activation may not enhance apoptotic cell death in postmitotic cortical neurons.

Since mTOR activity is upregulated in many types of human neurodegenerative diseases, we examined the possible involvement of the mTORC1 pathway in neurodegeneration.

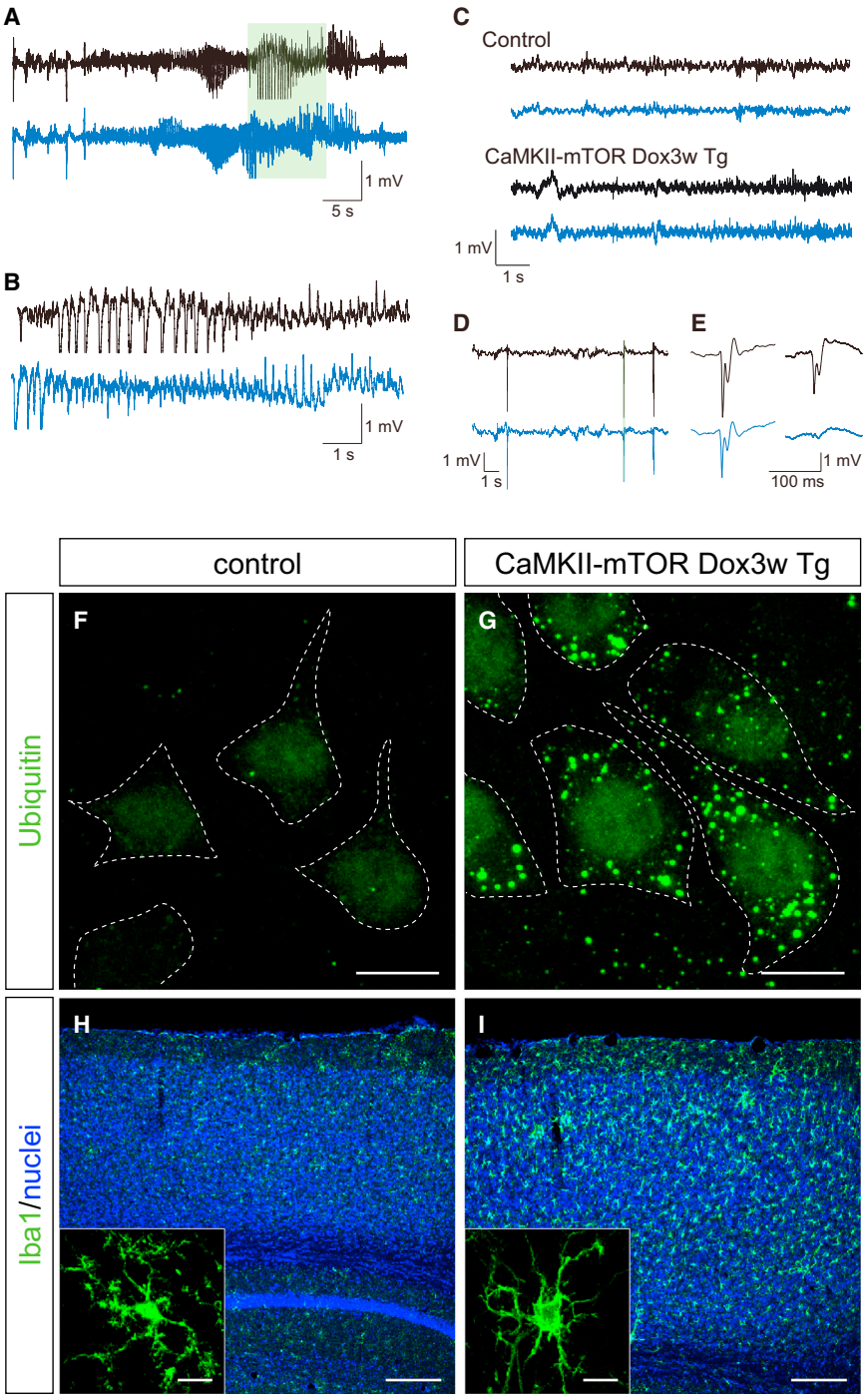

Figure 7. Epileptic Seizure and Neurodegeneration in CaMKII-mTOR Dox3w Tg Mice

(A–E) Epileptic seizure in CaMKII-mTOR Dox3w Tg mice.

(A and B) LFPs recorded from freely moving CaMKII-mTOR Dox3w Tg mice at 7 weeks of age during seizures. The sections of LFP traces shaded by a green rectangle in (A) are enlarged in (B). A clear difference in LFP between the right and left hemispheres was observed during seizures.

(C) LFPs recorded from freely moving control and CaMKII-mTOR Dox3w Tg mice during exploration. Black and blue traces represent LFPs of right and left parietal cortices, respectively. No difference was observed in synchronous theta oscillations between the two genotypes.

(D and E) Frequent bilateral large interictal spikes in CaMKII-mTOR Dox3w Tg mice. Bilateral large interictal spikes indicated by green rectangles in (D) consist of sharp spikes and waves in left traces in (E).

(E) Variable types of interictal spikes observed in CaMKII-mTOR Dox3w Tg mice. Both bilateral (left traces) and unilateral (right traces) interictal spikes were observed in the single CaMKII-mTOR Dox3w Tg mouse.

(F–I) Neurodegeneration in CaMKII-mTOR Dox3w Tg cortex.

(F and G) Cortical sections from control and CaMKII-mTOR Dox3w Tg mice at 7 weeks of age were stained with an antibody against ubiquitin (green). Accumulation of ubiquitin-positive cytoplasmic inclusions was readily detectable in CaMKII-mTOR Dox3w Tg mice (G). Dotted lines depict boundaries of individual neurons.

(H and I) Microglial cells in the cerebral cortex were stained with an antibody against Iba1 (green), a marker of microglial cells. Cell nuclei were stained with TO-PRO-3 (blue). Characteristic changes in morphology of microglial cells were observed in CaMKII-tTA Dox3w Tg mice with enlarged cell bodies and short protrusions (I). Inset: high-power images of microglial cells.

Scale bars, 10 μm (F, G, and inset in H and I) and 200 μm (H and I). See also Figures S5–S7 and Movies S1, S2, S3, and S4.

We stained cortical sections from control and CaMKII-mTOR Dox3w Tg mice with anti-ubiquitin antibody, which can identify cytoplasmic inclusions, a characteristic feature of neurodegeneration. In CaMKII-mTOR Dox3w Tg cortex, a large number of ubiquitin-positive cytoplasmic inclusions were found in many neurons, especially in the pyramidal neurons in layers II/III and V (Figure 7G), whereas ubiquitin-positive inclusions were rarely detected in the control cortex (Figure 7F). Rapid accumulation of cytoplasmic inclusions was also found in CaMKII-mTOR Dox(−) Tg mice at P12 (Figures S7A and S7B), indicative of involvement of mTORC1 signaling in neurodegeneration.

Microglial cells are resident immune cells in the CNS and are involved in the pathogenesis of neurodegenerative diseases as well as in the engulfment of damaged cells (Perry et al., 2010). They undergo increased proliferation and drastic morphological changes in response to neuronal degeneration or inflammation. We examined the activation of microglial cells by staining cortical sections with Iba1, a microglial cell marker. Microglial cells in the control cortex showed relatively normal-sized cell bodies with

highly branched protrusions (Figures 7H and S7C). In contrast, we found an increased number of microglial cells with enlarged cell bodies and short processes in both CaMKII-mTOR Dox3w Tg and CaMKII-mTOR Dox(−) Tg cortices (Figures 7I and S7D), indicating that activation of microglial cells is associated with neurodegeneration. These results support the notion that activation of the mTORC1 pathway in postmitotic neurons accelerates the accumulation of cytoplasmic inclusions, faithfully recapitulating neurodegenerative diseases.

DISCUSSION

Since the brain is one of the most energy-consuming organs in the body, mTOR has been assumed to play an important role in neuronal functions. Aberrant activation of mTOR signaling in the CNS has been implicated in many human neurological diseases and has attracted considerable attention as a potential therapeutic target using rapamycin analogs. Recently, several mouse models for constitutive activation of mTOR signaling have been generated by conditional deletion of either the *Tsc1* or *Tsc2* gene. In the embryonic cerebral cortex, hyperactivation of mTOR signaling by deletion of *Tsc1* leads to enhanced proliferation of SVZ progenitors and cortical hypertrophy (Carson et al., 2012; Magri et al., 2011). These phenotypes contrast starkly with those observed in our Emx1-mTOR Tg mice, which exhibited prominent apoptosis of cortical SVZ progenitors but normal proliferation during corticogenesis. A reduction in the number of SVZ progenitors may deplete the progenitor pool, resulting in cortical atrophy in adulthood. One possible explanation for the discrepancy between these phenotypes is that the activation level of mTOR signaling may differ between conditional *Tsc1* knockout and Emx1-mTOR Tg mice. In conditional *Tsc1* knockout mice, the activation level of mTOR signaling critically depends on the expression level of endogenous mTOR kinase, and thus its activation may vary in different brain regions and developmental periods. In contrast, we were able to directly activate the mTORC1 pathway in a spatiotemporally controlled manner by using active mTOR kinase in our Tg mice. Therefore, the molecular and physiological phenotypes observed in this study can be attributed largely to hyperactivation of the mTORC1 pathway.

Although mTOR has a cell-protective function in general, inappropriate activation of mTOR signaling can make cells sensitive to apoptosis, especially quiescent cells such as neurons. In fact, microcephaly-capillary malformation syndrome is caused by a mutation in the *STAMBP* gene, which is associated with aberrant activation of the mTORC1 pathway and apoptotic cell death (McDonell et al., 2013). TUNEL-positive apoptotic cells have been detected in cortical tubers from human patients with TSC (Maldonado et al., 2003), as well as in the mouse model of TSC (Zeng et al., 2007). However, the molecular mechanism that underlies apoptotic neuronal cell death by mTORC1 activation is largely unknown. We identified HIF-1α as a potential downstream target that triggered apoptosis of neuronal progenitors in Emx1-mTOR Tg cortex. Activated mTOR upregulated HIF-1α expression, presumably by enhanced protein synthesis and/or stabilization by direct interaction with the mTORC1 complex through the TOS motif of HIF-1α. Furthermore, we confirmed elevated expression of p21, a downstream HIF-1 target gene that is involved in cell-cycle control. It was previously demonstrated that during hypoxia, enhanced activation of HIF-1α by mTORC1 could be reversed by treatment with rapamycin (Land and Tee, 2007). In line with these observations, genetic studies using embryonic stem cells lacking HIF-1α also showed decreased levels of apoptosis (Carmeliet et al., 1998). Therefore, HIF-1 signaling may provide a possible mechanistic link between apoptosis of neuronal cells and mTORC1 signaling.

In contrast to the cortical atrophy observed in Emx1-mTOR Tg mice, mTORC1 activation in postmitotic neurons induced cortical hypertrophy and increased neuronal cell size in CaMKII-mTOR Tg mice. Previous studies showed that suppression of DISC1, the schizophrenia susceptibility gene, perturbs neuronal development and cell size regulation via hyperactivation of the mTORC1 pathway (Kim et al., 2009). Abnormal activation of mTOR signaling has been detected in cytomegalic neurons of patients with TSC (Orlova and Crino, 2010) or cortical dysplasia (Ljungberg et al., 2006). More recently, de novo somatic mutations of mTOR (C1483Y) were identified in a patient with hemimegalencephaly, a rare congenital disorder characterized by overgrowth of one-half of the brain (Lee et al., 2012). Pathological samples from the affected patient showed elevated phosphorylation of S6 protein, suggesting that the C1483Y mutation is a novel spontaneous gain-of-function mutation of mTOR. In contrast, inactivation of mTORC1 in the developing brain was shown to cause a reduction in cell size and number, resulting in microcephaly in late embryogenesis (Cloëtta et al., 2013). Together with these studies, our data support the notion that cortical hypertrophy and enlarged neurons are caused by gain of function of mTORC1 signaling.

Generally, epileptic seizures are associated with human neurological diseases that involve structural abnormalities in the brain. In TSC, cortical tubers that include ectopic neurons with abnormal morphology and migration are assumed to serve as the foci of epileptic seizures. In this work, although the CaMKII-mTOR Dox3w Tg mice experienced fatal epileptic seizures, they did not form any detectable cortical tuber-like structures. It is possible that intracranial hypertension due to cortical hypertrophy may cause epileptic seizures in CaMKII-mTOR Dox3w Tg mice. In the cortex of *Tsc1* conditional knockout mice, both abnormal brain structure and epileptic seizures could be suppressed by rapamycin treatment, but epileptic seizures recurred shortly after withdrawal of rapamycin without structural abnormalities of the brain (Magri et al., 2011). *Pten* deletion in adult-generated granule neurons of the hippocampal dentate gyrus hyperactivates mTOR signaling and drives aberrant circuit formation during epileptogenesis (Pun et al., 2012). Therefore, it may also be possible that deregulation of synaptic activity and neural circuit formation by aberrant activation of mTOR signaling are involved in induction of epileptic seizures.

In parallel with cortical hypertrophy and epilepsy, we observed neurodegenerative disease-like symptoms in the cortical neurons of both CaMKII-mTOR Dox(−) Tg and CaMKII-mTOR Dox3wTg mice. Accumulation of cytoplasmic inclusions accompanied by neurodegeneration has been also detected in cortical neurons and cerebellar Purkinje cells in mice lacking the

autophagy-related gene *Atg5* (Hara et al., 2006) or *Atg7* (Komatsu et al., 2006). Autophagy is a bulk protein degradation process, and activation of mTORC1 crucially suppresses the formation of autophagosomes by phosphorylating ULK1 and Atg13, resulting in the accumulation of various aggregate-prone proteins (Mizushima and Komatsu, 2011). However, the onset of cytoplasmic accumulation occurs much later in autophagy-deficient mice than in CaMKII-mTOR Dox(−) Tg mice. In addition to the suppression of autophagy, enhanced protein synthesis by mTORC1 activation may accelerate the onset of accumulation of the cytoplasmic inclusions in CaMKII-mTOR Dox(−) Tg mice. Alternatively, epileptic seizure may induce neurodegeneration by currently unknown mechanisms. Since epileptic seizure has been implicated in neuronal cell death (Pitkänen and Lukasiuk, 2011), the frequent seizures in CaMKII-mTOR Dox(−) Tg mice may promote a progression of neurodegeneration, which in turn deteriorates epileptic seizures.

Our findings suggest that mTOR signaling in the CNS adopts different downstream effectors for neuronal survival during the embryonic and adult stages. Such stage-specific functional differences in mTOR signaling may contribute to a wide range of neurological diseases. In principle, the mutant mice generated in this study can be applicable to every tissue and cell type, and therefore will provide a better understanding of the molecular mechanisms of mTOR-related human diseases.

EXPERIMENTAL PROCEDURES

Generation of Tg Mice

The animal experiments were conducted in accordance with the guidelines of The University of Tokyo. The active mutant of rat mTOR kinase was isolated as described previously (Ohne et al., 2008). For *CAG-mTOR^{SL1+IT}* Tg mice, a transgene was constructed by inserting the *mTOR^{SL1+IT}* mutant into the pCALNL5 vector, which directs gene expression under the control of the CAG promoter in response to Cre-*loxP* recombination (Figure 1A). For *TRE-mTOR^{SL1+IT}* Tg mice, the *mTOR^{SL1+IT}* mutant was placed downstream of TRE, and the chicken *β-globin* insulator sequence was introduced at the 5′ ends of the transgene (Figure 4A). These transgenes were linealized and separately injected into the pronuclei of C57BL/6 embryos. Founder Tg mice were crossed with C57BL/6 mice, and the established Tg mice were genotyped by genomic PCR analysis using a pair of primers designed to amplify the portion of rat mTOR gene (5′-CAAGG ATGAC GACGA TAAGG-3′ and 5′-TGCCA TCTCC ATGAC AACTG-3′). Emx1-cre knockin mice were generated as described previously (Kassai et al., 2008). CaMKII-tTA Tg mice were obtained from The Jackson Laboratory (Mayford et al., 1996). The genetic background of the Tg mice used in this study was a hybrid of C57BL/6, DBA/2, and ICR. We confirmed that Tg mice with the C57BL/6 background gave essentially the same results.

Drug Administration

Doxycycline hyclate (Sigma) was dissolved in drinking water (200 mg/l) and supplied to pups and their parents until 3 weeks of age. Rapamycin (R-5000; LC Laboratories) was prepared as a 25 mg/ml stock solution in ethanol. Before each administration, the stock solution was diluted in 5% Tween-80, 5% polyethylene glycol 400 (0.5–1.5 mg/ml). Rapamycin was given at 5 mg/kg intraperitoneally once per day for more than 4 weeks from 3 weeks of age.

Western Blot Analysis

Western blot analysis was performed as described previously (Kassai et al., 2008). Additional details of the methods and antibodies used can be found in Supplemental Experimental Procedures.

Histology

Histological analysis was performed as described previously (Kassai et al., 2008). Supplemental Experimental Procedures contains detailed information regarding Nissl staining, β-galactosidase staining, and immunohistochemical analysis.

In Utero Electroporation

The protocols used for in utero electroporation experiments are detailed in Supplemental Experimental Procedures.

LFP Recording in Freely Moving Mice

For LFP recording, we used immature and adult CaMKII-mTOR Tg mice and their control littermates. The immature mice were P15 on the day of electrode implantation and adult mice were 7 weeks old, which corresponds to the timing 4 weeks after withdrawal of doxycycline. Under isoflurane anesthesia (1.5%), recording electrodes (polyurethane-coated stainless-steel wire with 100 μm in diameter) were placed on the bilateral parietal cortex (1 mm lateral, 1 mm posterior to bregma for immature mice, and 2 mm lateral, 2 mm posterior to bregma for adult mice). Two microscrews with cables were positioned in the occipital bone. One was used as a ground and the other was used as an indifferent electrode. Electrodes were fixed to the skull with dental acrylic cement. Body temperature was maintained at 37°C throughout the surgery with the use of a heating blanket. Four days after implantation, the LFPs of bilateral parietal cortex were recorded in freely moving mice for 2 hr per day until the mice died. Signals were amplified (MEG-5200; Nihon-Koden) and digitized (PowerLab; AD Instruments) for analysis with the use of MATLAB (The MathWorks).

SUPPLEMENTAL INFORMATION

Supplemental Information includes Supplemental Experimental Procedures, seven figures, and four movies and can be found with this article online at http://dx.doi.org/10.1016/j.celrep.2014.04.048.

ACKNOWLEDGMENTS

We thank Drs. Shigeo Okabe (The University of Tokyo) and Makoto Sato (Osaka University) for providing valuable advice and plasmids for in utero electroporation experiments. We also thank Drs. Terunao Takahara and Yoichiro Ohne for helpful discussions. This study was supported in part by Grants-in-Aid for Scientific Research (22300106 to A.A., 21220006 and 25000015 to M.K., and 25291042 to T.M.) and for Young Scientists (B) (23700368 to H.K.) from the Japan Society for the Promotion of Science. This study was also partially supported by the Strategic Research Program for Brain Sciences (Development of Biomarker Candidates for Social Behavior), MEXT, Japan.

Received: August 14, 2013
Revised: March 18, 2014
Accepted: April 22, 2014
Published: May 22, 2014

REFERENCES

Bebin, E.M., Kelly, P.J., and Gomez, M.R. (1993). Surgical treatment for epilepsy in cerebral tuberous sclerosis. Epilepsia *34*, 651–657.

Bové, J., Martínez-Vicente, M., and Vila, M. (2011). Fighting neurodegeneration with rapamycin: mechanistic insights. Nat. Rev. Neurosci. *12*, 437–452.

Busquets-Garcia, A., Gomis-González, M., Guegan, T., Agustín-Pavón, C., Pastor, A., Mato, S., Pérez-Samartín, A., Matute, C., de la Torre, R., Dierssen, M., et al. (2013). Targeting the endocannabinoid system in the treatment of fragile X syndrome. Nat. Med. *19*, 603–607.

Carmeliet, P., Dor, Y., Herbert, J.M., Fukumura, D., Brusselmans, K., Dewerchin, M., Neeman, M., Bono, F., Abramovitch, R., Maxwell, P., et al. (1998). Role of HIF-1α in hypoxia-mediated apoptosis, cell proliferation and tumour angiogenesis. Nature *394*, 485–490.

Carson, R.P., Van Nielen, D.L., Winzenburger, P.A., and Ess, K.C. (2012). Neuronal and glia abnormalities in *Tsc1*-deficient forebrain and partial rescue by rapamycin. Neurobiol. Dis. *45*, 369–380.

Cloëtta, D., Thomanetz, V., Baranek, C., Lustenberger, R.M., Lin, S., Oliveri, F., Atanasoski, S., and Rüegg, M.A. (2013). Inactivation of mTORC1 in the developing brain causes microcephaly and affects gliogenesis. J. Neurosci. *33*, 7799–7810.

Cornu, M., Albert, V., and Hall, M.N. (2013). mTOR in aging, metabolism, and cancer. Curr. Opin. Genet. Dev. *23*, 53–62.

Groszer, M., Erickson, R., Scripture-Adams, D.D., Lesche, R., Trumpp, A., Zack, J.A., Kornblum, H.I., Liu, X., and Wu, H. (2001). Negative regulation of neural stem/progenitor cell proliferation by the *Pten* tumor suppressor gene in vivo. Science *294*, 2186–2189.

Gwinn, D.M., Shackelford, D.B., Egan, D.F., Mihaylova, M.M., Mery, A., Vasquez, D.S., Turk, B.E., and Shaw, R.J. (2008). AMPK phosphorylation of raptor mediates a metabolic checkpoint. Mol. Cell *30*, 214–226.

Hara, T., Nakamura, K., Matsui, M., Yamamoto, A., Nakahara, Y., Suzuki-Migishima, R., Yokoyama, M., Mishima, K., Saito, I., Okano, H., and Mizushima, N. (2006). Suppression of basal autophagy in neural cells causes neurodegenerative disease in mice. Nature *441*, 885–889.

Jaworski, J., and Sheng, M. (2006). The growing role of mTOR in neuronal development and plasticity. Mol. Neurobiol. *34*, 205–219.

Kassai, H., Terashima, T., Fukaya, M., Nakao, K., Sakahara, M., Watanabe, M., and Aiba, A. (2008). Rac1 in cortical projection neurons is selectively required for midline crossing of commissural axonal formation. Eur. J. Neurosci. *28*, 257–267.

Kim, J.Y., Duan, X., Liu, C.Y., Jang, M.H., Guo, J.U., Pow-anpongkul, N., Kang, E., Song, H., and Ming, G.L. (2009). DISC1 regulates new neuron development in the adult brain via modulation of AKT-mTOR signaling through KIAA1212. Neuron *63*, 761–773.

Komatsu, M., Waguri, S., Chiba, T., Murata, S., Iwata, J., Tanida, I., Ueno, T., Koike, M., Uchiyama, Y., Kominami, E., and Tanaka, K. (2006). Loss of autophagy in the central nervous system causes neurodegeneration in mice. Nature *441*, 880–884.

Land, S.C., and Tee, A.R. (2007). Hypoxia-inducible factor 1α is regulated by the mammalian target of rapamycin (mTOR) via an mTOR signaling motif. J. Biol. Chem. *282*, 20534–20543.

Laplante, M., and Sabatini, D.M. (2012). mTOR signaling in growth control and disease. Cell *149*, 274–293.

Lee, J.H., Huynh, M., Silhavy, J.L., Kim, S., Dixon-Salazar, T., Heiberg, A., Scott, E., Bafna, V., Hill, K.J., Collazo, A., et al. (2012). De novo somatic mutations in components of the PI_3K-AKT3-mTOR pathway cause hemimegalencephaly. Nat. Genet. *44*, 941–945.

Ljungberg, M.C., Bhattacharjee, M.B., Lu, Y., Armstrong, D.L., Yoshor, D., Swann, J.W., Sheldon, M., and D'Arcangelo, G. (2006). Activation of mammalian target of rapamycin in cytomegalic neurons of human cortical dysplasia. Ann. Neurol. *60*, 420–429.

Magri, L., Cambiaghi, M., Cominelli, M., Alfaro-Cervello, C., Cursi, M., Pala, M., Bulfone, A., Garcìa-Verdugo, J.M., Leocani, L., Minicucci, F., et al. (2011). Sustained activation of mTOR pathway in embryonic neural stem cells leads to development of tuberous sclerosis complex-associated lesions. Cell Stem Cell *9*, 447–462.

Maldonado, M., Baybis, M., Newman, D., Kolson, D.L., Chen, W., McKhann, G., 2nd, Gutmann, D.H., and Crino, P.B. (2003). Expression of ICAM-1, TNF-α, NFκB, and MAP kinase in tubers of the tuberous sclerosis complex. Neurobiol. Dis. *14*, 279–290.

Mayford, M., Bach, M.E., Huang, Y.Y., Wang, L., Hawkins, R.D., and Kandel, E.R. (1996). Control of memory formation through regulated expression of a CaMKII transgene. Science *274*, 1678–1683.

McDonell, L.M., Mirzaa, G.M., Alcantara, D., Schwartzentruber, J., Carter, M.T., Lee, L.J., Clericuzio, C.L., Graham, J.M., Jr., Morris-Rosendahl, D.J., Polster, T., et al.; FORGE Canada Consortium. (2013). Mutations in *STAMBP*, encoding a deubiquitinating enzyme, cause microcephaly-capillary malformation syndrome. Nat. Genet. *45*, 556–562.

Meikle, L., Talos, D.M., Onda, H., Pollizzi, K., Rotenberg, A., Sahin, M., Jensen, F.E., and Kwiatkowski, D.J. (2007). A mouse model of tuberous sclerosis: neuronal loss of *Tsc1* causes dysplastic and ectopic neurons, reduced myelination, seizure activity, and limited survival. J. Neurosci. *27*, 5546–5558.

Mizushima, N., and Komatsu, M. (2011). Autophagy: renovation of cells and tissues. Cell *147*, 728–741.

Ohne, Y., Takahara, T., Hatakeyama, R., Matsuzaki, T., Noda, M., Mizushima, N., and Maeda, T. (2008). Isolation of hyperactive mutants of mammalian target of rapamycin. J. Biol. Chem. *283*, 31861–31870.

Orlova, K.A., and Crino, P.B. (2010). The tuberous sclerosis complex. Ann. N Y Acad. Sci. *1184*, 87–105.

Perry, V.H., Nicoll, J.A., and Holmes, C. (2010). Microglia in neurodegenerative disease. Nat. Rev. Neurol. *6*, 193–201.

Pitkänen, A., and Lukasiuk, K. (2011). Mechanisms of epileptogenesis and potential treatment targets. Lancet Neurol. *10*, 173–186.

Pun, R.Y., Rolle, I.J., Lasarge, C.L., Hosford, B.E., Rosen, J.M., Uhl, J.D., Schmeltzer, S.N., Faulkner, C., Bronson, S.L., Murphy, B.L., et al. (2012). Excessive activation of mTOR in postnatally generated granule cells is sufficient to cause epilepsy. Neuron *75*, 1022–1034.

Ravikumar, B., Vacher, C., Berger, Z., Davies, J.E., Luo, S., Oroz, L.G., Scaravilli, F., Easton, D.F., Duden, R., O'Kane, C.J., and Rubinsztein, D.C. (2004). Inhibition of mTOR induces autophagy and reduces toxicity of polyglutamine expansions in fly and mouse models of Huntington disease. Nat. Genet. *36*, 585–595.

Reith, R.M., Way, S., McKenna, J., 3rd, Haines, K., and Gambello, M.J. (2011). Loss of the tuberous sclerosis complex protein tuberin causes Purkinje cell degeneration. Neurobiol. Dis. *43*, 113–122.

Sancak, Y., Thoreen, C.C., Peterson, T.R., Lindquist, R.A., Kang, S.A., Spooner, E., Carr, S.A., and Sabatini, D.M. (2007). PRAS40 is an insulin-regulated inhibitor of the mTORC1 protein kinase. Mol. Cell *25*, 903–915.

Sato, A., Kasai, S., Kobayashi, T., Takamatsu, Y., Hino, O., Ikeda, K., and Mizuguchi, M. (2012). Rapamycin reverses impaired social interaction in mouse models of tuberous sclerosis complex. Nat. Commun. *3*, 1292.

Sharma, A., Hoeffer, C.A., Takayasu, Y., Miyawaki, T., McBride, S.M., Klann, E., and Zukin, R.S. (2010). Dysregulation of mTOR signaling in fragile X syndrome. J. Neurosci. *30*, 694–702.

Sharp, F.R., and Bernaudin, M. (2004). HIF1 and oxygen sensing in the brain. Nat. Rev. Neurosci. *5*, 437–448.

Swiech, L., Perycz, M., Malik, A., and Jaworski, J. (2008). Role of mTOR in physiology and pathology of the nervous system. Biochim. Biophys. Acta *1784*, 116–132.

Tsai, P.T., Hull, C., Chu, Y., Greene-Colozzi, E., Sadowski, A.R., Leech, J.M., Steinberg, J., Crawley, J.N., Regehr, W.G., and Sahin, M. (2012). Autistic-like behaviour and cerebellar dysfunction in Purkinje cell *Tsc1* mutant mice. Nature *488*, 647–651.

Vander Haar, E., Lee, S.I., Bandhakavi, S., Griffin, T.J., and Kim, D.H. (2007). Insulin signalling to mTOR mediated by the Akt/PKB substrate PRAS40. Nat. Cell Biol. *9*, 316–323.

Wang, L., Harris, T.E., Roth, R.A., and Lawrence, J.C., Jr. (2007). PRAS40 regulates mTORC1 kinase activity by functioning as a direct inhibitor of substrate binding. J. Biol. Chem. *282*, 20036–20044.

Way, S.W., McKenna, J., 3rd, Mietzsch, U., Reith, R.M., Wu, H.C., and Gambello, M.J. (2009). Loss of *Tsc2* in radial glia models the brain pathology of tuberous sclerosis complex in the mouse. Hum. Mol. Genet. *18*, 1252–1265.

Wullschleger, S., Loewith, R., and Hall, M.N. (2006). TOR signaling in growth and metabolism. Cell *124*, 471–484.

Yamagata, K., Sanders, L.K., Kaufmann, W.E., Yee, W., Barnes, C.A., Nathans, D., and Worley, P.F. (1994). *rheb*, a growth factor- and synaptic

activity-regulated gene, encodes a novel Ras-related protein. J. Biol. Chem. *269*, 16333–16339.

Yang, S.B., Tien, A.C., Boddupalli, G., Xu, A.W., Jan, Y.N., and Jan, L.Y. (2012). Rapamycin ameliorates age-dependent obesity associated with increased mTOR signaling in hypothalamic POMC neurons. Neuron *75*, 425–436.

Zeng, L.H., Ouyang, Y., Gazit, V., Cirrito, J.R., Jansen, L.A., Ess, K.C., Yamada, K.A., Wozniak, D.F., Holtzman, D.M., Gutmann, D.H., and Wong, M. (2007). Abnormal glutamate homeostasis and impaired synaptic plasticity and learning in a mouse model of tuberous sclerosis complex. Neurobiol. Dis. *28*, 184–196.

Zhou, J., Shrikhande, G., Xu, J., McKay, R.M., Burns, D.K., Johnson, J.E., and Parada, L.F. (2011). *Tsc1* mutant neural stem/progenitor cells exhibit migration deficits and give rise to subependymal lesions in the lateral ventricle. Genes Dev. *25*, 1595–1600.

Zou, J., Zhou, L., Du, X.X., Ji, Y., Xu, J., Tian, J., Jiang, W., Zou, Y., Yu, S., Gan, L., et al. (2011). Rheb1 is required for mTORC1 and myelination in postnatal brain development. Dev. Cell *20*, 97–108.